Deterministic phase measurements exhibiting super-sensitivity and super-resolution

Schäfermeier, Clemens; Ježek, Miroslav; Madsen, Lars S.; Gehring, Tobias; Andersen, Ulrik Lund

Published in:
Optica

Link to article, DOI:
10.1364/OPTICA.5.000060

Publication date:
2018

Document Version
Publisher's PDF, also known as Version of record

Research Article Vol. 5, No. 1 / January 2018 / Optica 60

Deterministic phase measurements exhibiting super-sensitivity and super-resolution

Clemens Schäfermeier,[1,2,*] Miroslav Ježek,[3] Lars S. Madsen,[1,4] Tobias Gehring,[1] and Ulrik L. Andersen[1,5]

[1]Technical University of Denmark, Department of Physics, Fysikvej 309, 2800 Kongens Lyngby, Denmark
[2]Kavli Institute of Nanoscience, Delft University of Technology, 2628 CJ Delft, The Netherlands
[3]Department of Optics, Faculty of Science, Palacky University, 17. listopadu 1192/12, 77146 Olomouc, Czech Republic
[4]Currently at Centre for Engineered Quantum Systems, School of Mathematics and Physics, University of Queensland, St. Lucia, QLD 4072, Australia
[5]e-mail: ulrik.andersen@fysik.dtu.dk
*Corresponding author: clemens@fh-muenster.de

Received 28 August 2017; revised 8 December 2017; accepted 8 December 2017 (Doc. ID 305120); published 18 January 2018

Phase super-sensitivity is obtained when the sensitivity in a phase measurement goes beyond the quantum shot noise limit, whereas super-resolution is obtained when the interference fringes in an interferometer are narrower than half the input wavelength. Here we show experimentally that these two features can be simultaneously achieved using a relatively simple setup based on Gaussian states and homodyne measurement. Using 430 photons shared between a coherent and a squeezed vacuum state, we demonstrate a 22-fold improvement in the phase resolution, while we observe a 1.7-fold improvement in the sensitivity. In contrast to previous demonstrations of super-resolution and super-sensitivity, this approach is fully deterministic.

OCIS codes: (270.0270) Quantum optics; (270.6570) Squeezed states; (120.5050) Phase measurement.

https://doi.org/10.1364/OPTICA.5.000060

1. INTRODUCTION

Quantum interference of light plays a pivotal role in high-precision quantum sensing [1], optical quantum computation [2], and quantum state tomography [3]. It is typically understood as two-beam interference that can be observed, for instance, in a Mach–Zehnder interferometer or a double-slit experiment. At the output, such interferometers create an oscillatory pattern with a periodicity given by half of the wavelength ($\lambda/2$) of the radiation field, which may be referred to, in analogy to the resolution-benchmark in optical imaging, as the "Rayleigh criterion" for phase measurements. This limit can, however, be surpassed using different types of states or measurement schemes [4–10]. In particular, measurement schemes that are based on parity detection [9,11] or approximate parity detection via a phase-space relation [8] are utilized to beat this limit with classical states, i.e., they do not require quantum states [12]. The arguably best-known quantum approach to observe a fringe narrowing uses NOON states, $|\psi\rangle \propto |N,0\rangle + e^{iN\phi}|0,N\rangle$. Surpassing the Rayleigh criterion is referred to as super-resolution [13,14] and is studied in the context of, e.g., optical lithography [5], matter-wave interferometry [15], and radar ranging [16].

In quantifying the performance for applications in quantum sensing and imaging, it is common to evaluate the Fisher information [17], or, equivalently, determine the sensitivity in the interferometric phase measurement. Using coherent states of light the optimal sensitivity is given by $1/\sqrt{N}$, where N is the mean number of photons of the state [18]. This sensitivity constitutes the shot noise limit (SNL). Overcoming the SNL is commonly referred to as super-sensitivity and can be achieved by nonclassical states [1,19–21]. Super-sensitivity based on squeezed states of light has proven to be a powerful and practical way to enhance the sensitivity of gravitational wave detectors [22,23].

The effects of super-sensitivity and super-resolution can be obtained simultaneously. For example, optical NOON states offer a sensitivity with Heisenberg scaling, $1/N$, and a phase resolution that scales as $\lambda/2N$ corresponding to N fringes per half-wavelength. NOON states thus exhibit an equal scaling in the two effects. In contrast, this work shows how resolution and sensitivity are tuneable and can, in fact, compete with each other. Due to the high fragility of NOON states, the complexity in their generation, and the commonly probabilistic way of generation, super-sensitivity and super-resolution have been only measured in the coincidence basis and in a highly probabilistic setting [6,19,24,25]. It has also been suggested to use two-mode squeezed vacuum states in combination with parity detection to attain the two "super-features" simultaneously [26]. However, possibly due to the complications in implementing a parity detection scheme, it has so far never been achieved experimentally. The complexity associated with the two schemes are due to the involved non-Gaussian states (NOON states) or the non-Gaussian measurements (parity detection). A natural question to ask is whether the same "super-features" can be realized using simple Gaussian operations. Here we answer this question in the affirmative.

We propose and experimentally demonstrate that, by using Gaussian states of light and Gaussian measurements, it is possible to realize a phase measurement that features super-resolution and super-sensitivity simultaneously. Using displaced squeezed states of light in conjunction with homodyne detection followed by a data-windowing technique, we show that the interferometric fringes can be made arbitrarily narrow while at the same time beating the shot noise limit. In stark contrast to the NOON state scheme, which, in any practical setting, is highly probabilistic both in preparation and in detection, our approach provides a deterministic demonstration of super-resolution and super-sensitivity.

2. MATERIALS AND METHODS

An illustration of the basic scheme is shown in Fig. 1. A vacuum squeezed state is combined with a coherent state of light at the entrance to a symmetric Mach–Zehnder interferometer. The Wigner function at the input is given by

$$W_{\text{in}}(x_1,p_1,x_2,p_2) = W_{|\alpha\rangle}(x_1,p_1)\,W_{|\xi\rangle}(x_2,p_2) = \frac{2\exp(-2((x_1-\alpha)^2+p_1^2))}{\pi}\cdot\frac{2\mathcal{P}\exp\left(-2\left(\mathcal{P}^2\varsigma^2x_2^2+\frac{p_2^2}{\varsigma^2}\right)\right)}{\pi}, \quad (1)$$

where x_n and p_n are the amplitude- and phase-quadratures; α is the amplitude of the coherent state; and $\varsigma = e^{-r}$, where r denotes the squeezing parameter and $\mathcal{P}$ represents the purity of the squeezed state. In the scheme, an amplitude-modulated coherent state and a phase-squeezed vacuum state interfere on the first beam splitter of the interferometer. Then the resulting state acquires a relative phase shift $\Delta\phi$, next interferes on the second beam splitter, and finally, one of the outputs is measured. As we used weak input signals, a homodyne readout scheme was employed. Figure 1 illustrates the trajectory of the output state in phase space for different phase shifts.

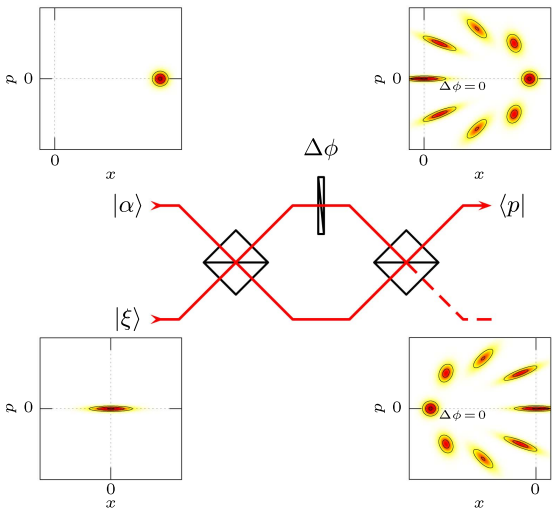

Fig. 1. Scheme of the approach. A coherent state $|\alpha\rangle$ and a vacuum squeezed state $|\xi\rangle$ are interfered on the first beam splitter. Insets show Wigner functions of the respective states, simulated for $\varsigma = \frac{1}{e}$ and $\alpha = 10$. In one of the resulting modes, a variable phase shifter is placed. At the second beam splitter the modes interfere again, producing the depicted Wigner functions. Eight superimposed distributions illustrate the effect of the phase shift, that is, each distribution is separated by $\frac{\pi}{4}$. If at $\Delta\phi = 0$ the squeezed vacuum state leaves the upper arm, the coherent state exits the lower one. Finally, the state is projected onto the quadrature eigenstate $\langle p|$ and partitioned by $\hat{\Pi}$.

If the interferometer is operated near a dark fringe, i.e., biasing the phase shift such that most of the light exits the second output of the interferometer, the phase-squeezed vacuum state will be detected. Thereby, the shot noise around the bias is suppressed and the phase sensitivity improved. The approach of feeding the commonly unused input mode with a vacuum squeezed state is equal to the proposal by Caves [20] to beat the shot noise limit in phase measurements. However, since the phase response for Caves' scheme reads $N\cos^2(\phi/2)$, which is an oscillating function with a period equal to $\lambda/2$, the resolution coincides with the mentioned "Rayleigh criterion" for phase measurements. In the following we show that by implementing a homodyne windowing scheme, the setup yields super-resolution and super-sensitivity.

The quadrature measurement of the homodyne detector is divided into two bins set by the "bin size" a: if the phase quadrature $\hat{p}$ is measured, we categorize two different results, which are associated with the intervals $|p| \le a$ and $|p| > a$. We describe such a measurement strategy by the projectors

$$\hat{\Pi}_0 = \int_{-a}^{a} \mathrm{d}p|p\rangle\langle p|, \quad \hat{\Pi}_1 = \hat{I} - \hat{\Pi}_0. \quad (2)$$

The measurement observable can thus be written as $\hat{\Pi} = \lambda_0\hat{\Pi}_0 + \lambda_1\hat{\Pi}_1$, where $\lambda_0 = 1/\mathrm{erf}(\sqrt{2}a)$ and $\lambda_1 = 0$ are the eigenvalues associated with the two measurement outcomes. Now the detector response is found by evaluating $\langle\hat{\Pi}\rangle$, which, in the idealized case of $\hat{\Pi} = |p=0\rangle\langle p=0|$, i.e., $a \to 0$, and a pure squeezed vacuum state, yields

$$\langle\hat{\Pi}\rangle_{a\to 0,\mathcal{P}=1} = \frac{2\varsigma^2\exp\left(-\frac{2\varsigma^2|\alpha|^2\sin^2\phi}{2\varsigma^2(\varsigma^2-1)\cos\phi+(\varsigma^4-1)\cos^2\phi+(\varsigma^2+1)^2}\right)}{\sqrt{(\varsigma^4-1)\cos^2\phi+2(\varsigma^2-1)\varsigma^2\cos\phi+(\varsigma^2+1)^2}}. \quad (3)$$

The full width half-maximum (FWHM) of this function follows $1/|\alpha|$ for $|\alpha| \to \infty$, thereby indicating that the interference fringes become narrower as α is increasing and thus demonstrating super-resolution. It should be stressed that setting $a = 0$ is an idealization, as it means a projection on an infinitely squeezed state, i.e., even-number state. However, it points out that the operator $\hat{\Pi}$ is in some sense an approximation of the parity operator [9,11]. Considering instead a realistic setting where $a \neq 0$ and the squeezed state is not pure ($\mathcal{P} < 1$), the response function reads

$$\langle\hat{\Pi}\rangle = \frac{1}{2\,\mathrm{erf}\left(\frac{\sqrt{2}a}{\varsigma}\right)}\left[\mathrm{erf}\left(\sqrt{\frac{2}{c_1}}c_-\right)+\mathrm{erf}\left(\sqrt{\frac{2}{c_1}}c_+\right)\right], \quad (4)$$

where

$$c_\pm = a \pm \frac{1}{2}|\alpha|\sin\phi$$

and

$$c_1 = \frac{\mathcal{P}^2\varsigma^2(\varsigma^2(\cos\phi+1)^2+2(1-\cos\phi))-\cos^2\phi+1}{4\mathcal{P}^2\varsigma^2}. \quad (5)$$

The scaling of the FWHM is preserved for a general value a, i.e., FWHM $\propto 1/|\alpha|$. In Fig. 2(a) we plot the FWHM improvement as a function of the squeezing parameter ς and the bin size a. It is clear from this plot that the super-resolution

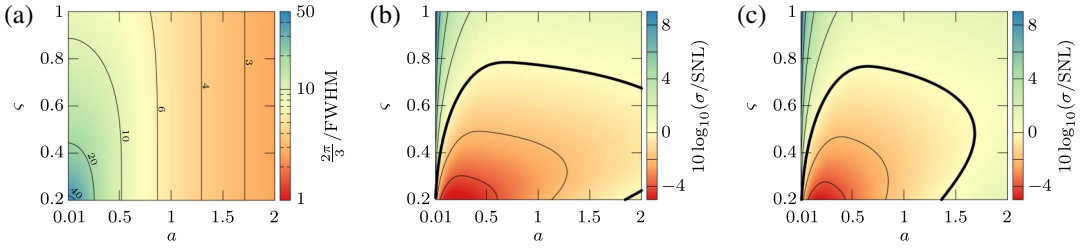

Fig. 2. Performance of the protocol for $\alpha = 10$ under variation of the bin size and squeezing parameter. (a) Improvement of the FWHM compared to the Rayleigh criterion ($2\pi/3$). The achieved FWHM is extracted numerically from the response of a pure state. The improvement is monotonic in the sense that a smaller bin size a always leads to a higher resolution. (b) Maximum sensitivity compared to the SNL. The region with negative values describes the parameter space where the SNL is surpassed. The threshold is marked by the bold line. (c) Unlike case (b), we set the purity $\mathcal{P} = 1/2$.

feature only depends weakly on the degree of squeezing, and a similar conclusion is found for the purity of the state. The only critical parameter for attaining high resolution is the mean photon number of the input coherent state. More details and a derivation may be found in Supplement 1.

We now turn to the investigation of the sensitivity using the above scheme. The sensitivity can be found using the uncertainty propagation formula,

$$\sigma = \Delta\hat{\Pi}/|d/d\phi\langle\hat{\Pi}\rangle|, \tag{6}$$

where $\Delta\hat{\Pi} = \sqrt{\langle\hat{\Pi}^2\rangle - \langle\hat{\Pi}\rangle^2}$, and for our measurement operator it follows

$$\sigma = \Big|c_1^{\frac{3}{2}}\sqrt{(2-c_2)c_2\pi/2}/[\exp(-2c_-^2/c_1)(c_1'c_- + \alpha c_1\cos\phi) + \exp(-2c_+^2/c_1)(c_1'c_+ - \alpha c_1\cos\phi)]\Big|, \tag{7}$$

with the notations $c_1' = \frac{d}{d\phi}c_1$ and $c_2 = \mathrm{erf}\left(\sqrt{2/c_1}c_-\right) + \mathrm{erf}\left(\sqrt{2/c_1}c_+\right)$. For a specific parameter regime defined by the purity $\mathcal{P}$, the bin size a, and the squeezing parameter ς, this sensitivity beats the shot noise limit. In Figs. 2(b) and 2(c) we plot the sensitivity σ relative to the shot-noise-limited sensitivity as a function of the bin size and the squeezing parameter for two different purities. It is shown in Fig. 2(c) that it is possible to achieve super-sensitivity in a setting where the squeezed state is impure. In conclusion, both super-sensitivity and super-resolution can be achieved in a practical setup for the parameter space shown in Fig. 2(c). Furthermore, sensitivity and resolution features are neither independent nor fixed with respect to each other, but can be varied by the homodyne windowing technique. A discussion of the ultimate sensitivity may be found in Supplement 1.

We proceed by discussing the experimental realization depicted in Fig. 3. A squeezed vacuum state and a coherent state with a controllable photon number is injected into the input ports of a polarization-based Mach–Zehnder interferometer. The polarization basis ensures high stability and quality of the interference. Furthermore, it allows for simple control of the relative phase shift. The phase shift is varied by a half-wave plate mounted on a remote-controlled rotation stage. One output of the interferometer is measured with a high-efficiency homodyne detector exhibiting an overall quantum efficiency of 93%, given by 99% efficiency of the photo diodes and 97% visibility to the local oscillator (LO). The relative phase of the two input beams of the interferometer as well as the phase of the LO is actively stabilized via real-time feedback circuits, thereby recreating the scheme in

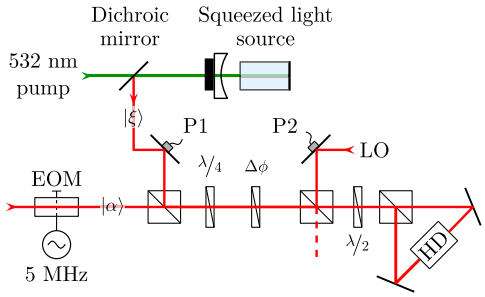

Fig. 3. Experimental implementation. A vacuum squeezed state, created by parametric downconversion, and a coherent state, generated via an electro-optic modulator (EOM), are sent into a polarization-based Mach–Zehnder interferometer (MZI). A quarter-wave plate in combination with a motorized half-wave plate ($\Delta\phi$) forms the equivalent phase shift of a MZI where the two modes are spatially separated. The piezo transducers P1 and P2 stabilize the phase between the input states and the local oscillator (LO), respectively. A half-wave plate in front of the last polarizing beam splitter is used to balance the photocurrent in the homodyne detector (HD). All cubes represent polarizing beam splitters.

Fig. 1 and projecting the output on the $\hat{p}$ quadrature. A detailed description may be found in Supplement 1.

A squeezed vacuum state is generated by parametric downconversion in a 10 mm long periodically poled potassium titanyl phosphate (KTP) crystal embedded in a 23.5 mm long cavity comprising a piezo-actuated curved mirror and a plane mirror integrated with end-facet of the crystal. A Pound–Drever–Hall (PDH) scheme is adopted to stabilize the cavity resonance. The downconversion process is pumped by a 45 mW continuous-wave laser beam operating at 532 nm, such that squeezed light is produced at 1064 nm. To stabilize the pump phase, the radio-frequency signal used also for cavity stabilization is down-mixed with a phase shift of 90°. Using a 5 mW local oscillator, we observe 6.5(1) dB shot noise suppression at 5 MHz sideband frequency, while the anti-squeezed quadrature is 11.3(1) dB above shot noise. The squeezed-state parameters read, on average, $\mathcal{P} = 0.58$ and $\varsigma = 0.47$. A complete characterization of the squeezed light source is presented in Supplement 1.

The coherent input state is produced by an electro-optical modulator (EOM) at a sideband frequency of 5 MHz. The chosen frequency ensures the creation of a coherent state far from low-frequency technical noise and with an amplitude $|\alpha|^2$ that is conveniently controlled by the modulation depth of the EOM.

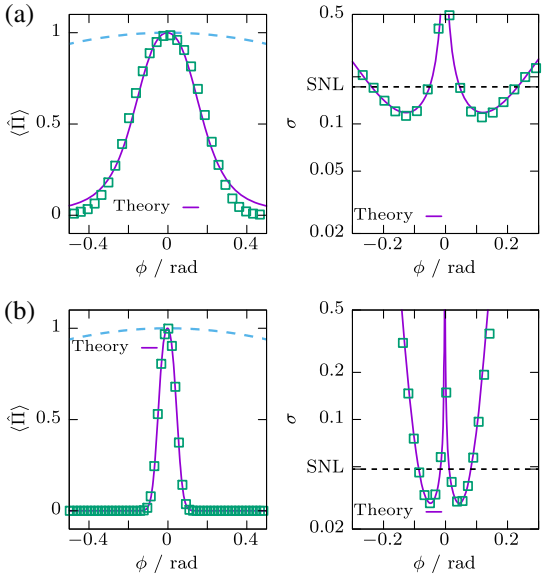

Fig. 4. Results achieved for an input state with (a) $|\alpha|^2 \approx 30.7$ ($N \approx 33.6$) and (b) $|\alpha|^2 \approx 427$ ($N \approx 430$). Left: The fringe after applying the dichotomy operator $\hat{\Pi}$. A dashed line follows the fringe of a standard interferometer. Its FWHM is (a) 5.7 and (b) 22.2 times larger compared to our result. Right: The sensitivity derived from the experimental data. In a range of about ± 0.1 rad, the SNL was surpassed by a factor of (a) 1.5 and (b) 1.7. The uncertainty of each data point is well within the "□" symbol. We attribute the symmetric deviations at the wings to a systematic anomaly in the set phase shift controlled by the HWP.

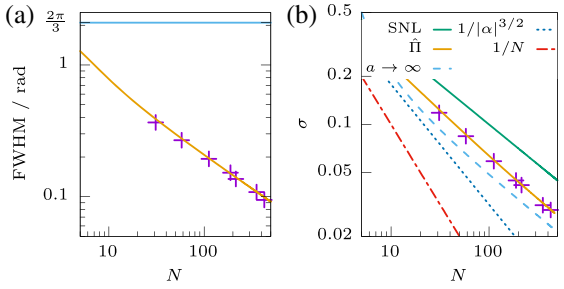

Fig. 5. Summary of experimental results. The solid orange lines are theoretical predictions derived from the measured squeezing parameters and displacement amplitude. Each cross symbolizes a measurement run. The uncertainties are much smaller than the symbol size. (a) The FWHM under variation of the total average photon number of the input state. It always beats the Rayleigh criterion of $2\pi/3$. Comparing the theoretically predicted FWHM proves a stable performance of the setup. (b) A comparison to four sensitivity limits. As for the resolution, the theoretical prediction affirms our experimental results. The SNL was outperformed throughout the experiment at a scaling of $N^{-0.56}$; the Heisenberg scaling of $1/N$ is, however, not attainable. Using no windowing ($a \to \infty$), a better sensitivity and a scaling of $N^{-0.57}$ can be achieved; however, it comes at the cost of super-resolution. The ultimate bound of our protocol follows $N^{-3/4}$, assuming no losses and restrictions on the squeezing degree.

To measure the interferometer's output state at 5 MHz, the electronic output of the homodyne detector is down-mixed at this frequency, subsequently low-pass filtered at 100 kHz, and then digitized with 14 bit resolution. For each phase setting, 10^6 samples are acquired at a sampling rate of 0.5 MHz. The data is recorded on a computer for post-processing that includes the dichotomic windowing strategy given by Eq. (2) in which we set the bin size $a = 1/2$. After dividing the data according to a, we calculate $\langle\hat{\Pi}\rangle$ as well as the standard deviation for each phase setting from the data. Finally, σ is computed according to Eq. (6). The term $\Delta\hat{\Pi}$ in Eq. (6) is extracted directly from the data. Instead of calculating the derivative of $\langle\hat{\Pi}\rangle$ also directly, it is estimated from the theoretical model of $\langle\hat{\Pi}\rangle$ fitted to the data. This approach is chosen to increase the confidence in the computation of σ, and a comparison between this and a direct evaluation is shown in Supplement 1. In the panels on the right of Fig. 4, σ is shown in comparison to the theoretical model given by Eq. (7).

3. RESULTS AND DISCUSSION

The results for a mean photon number of 33.6 and 430, with a mean of 2.8 photons contained in the squeezed state and an overall efficiency of circa 84%, are shown in Fig. 4 and compared with theoretical predictions. The latter is denoted by solid lines. It is clear from the plots that the scheme exhibits super-resolution as well as super-sensitivity for certain phase intervals. We expect that the resolution and sensitivity improves as the mean photon number is increased. This expectation is confirmed in Fig. 5 where the measurement of these two features for increasing photon numbers in the coherent state is depicted. Specifically, at $|\alpha|^2 = 427$ we obtain a 22-fold improvement in the phase resolution compared to a standard interferometer and a 1.7-fold improvement in the sensitivity relative to the shot noise limit.

It is interesting to compare these results with a scheme exploiting pure optical NOON states, which exhibit super-resolution and super-sensitivity at the same photon-number scaling. Using such states, a similar improvement in resolution and sensitivity would require a 23-photon and a 3-photon NOON state, respectively. Importantly, this only holds for a lossless scenario. As of today, an optical 5-photon NOON state has been produced which in principle will yield a 5-fold improvement in resolution and a 2.2-fold improvement in sensitivity [27]. However, this realization is intrinsically probabilistic and thus does not exhibit super-sensitivity in a deterministic setting. To the best of our knowledge, we found that the presented results constitute the first demonstration of super-resolution and super-sensitivity in a deterministic setting.

In summary, we proposed and experimentally demonstrated a simple approach to the simultaneous attainment of phase super-resolution and phase super-sensitivity. The approach is based on Gaussian squeezed states and Gaussian homodyne measurement followed by a windowing strategy, which is in stark contrast to previously proposed schemes realized with impractical and fragile NOON states, or high-efficiency parity detection. Our work is of fundamental interest as it highlights the fact that the observation of super-resolution is not a special quantum effect associated with non-Gaussian quantum states [6] or non-Gaussian measurements [7]. In conclusion, we find that the actual quantum feature—that is, super-sensitivity—may co-exist with the super-resolution feature without using advanced non-Gaussian states or non-Gaussian measurements. Assuming that the measurement's figure of merit is phase sensitivity, we cannot find an advantage in exploiting super-resolution in a Gaussian-noise-governed context. Furthermore,

we present the trade-off between resolution and sensitivity for the first time and show that significant super-resolution can be achieved at the cost of negligible increase of sensitivity at the scale of a fraction of SNL. This holds also in the presence of loss and classical Gaussian noise (discussed in Supplement 1). Our result sets a benchmark to evaluate super-resolving strategies, particularly under realistic imperfect conditions.

Funding. Lundbeckfonden; Det Frie Forskningsråd (DFF) (0602-01686B, 4184-00338B); Grantová Agentura České Republiky (GACR) (GB14-36681G).

See Supplement 1 for supporting content.

REFERENCES AND NOTE

1. V. Giovannetti, S. Lloyd, and L. Maccone, "Quantum-enhanced measurements: beating the standard quantum limit," Science **306**, 1330–1336 (2004).
2. P. Kok, W. J. Munro, K. Nemoto, T. C. Ralph, J. P. Dowling, and G. J. Milburn, "Linear optical quantum computing with photonic qubits," Rev. Mod. Phys. **79**, 135–174 (2007).
3. A. I. Lvovsky and M. G. Raymer, "Continuous-variable optical quantum-state tomography," Rev. Mod. Phys. **81**, 299–332 (2009).
4. J. G. Rarity, P. R. Tapster, E. Jakeman, T. Larchuk, R. A. Campos, M. C. Teich, and B. E. A. Saleh, "Two-photon interference in a Mach-Zehnder interferometer," Phys. Rev. Lett. **65**, 1348–1351 (1990).
5. A. N. Boto, P. Kok, D. S. Abrams, S. L. Braunstein, C. P. Williams, and J. P. Dowling, "Quantum interferometric optical lithography: exploiting entanglement to beat the diffraction limit," Phys. Rev. Lett. **85**, 2733–2736 (2000).
6. M. W. Mitchell, J. S. Lundeen, and A. M. Steinberg, "Super-resolving phase measurements with a multiphoton entangled state," Nature **429**, 161–164 (2004).
7. K. J. Resch, K. L. Pregnell, R. Prevedel, A. Gilchrist, G. J. Pryde, J. L. O'Brien, and A. G. White, "Time-reversal and super-resolving phase measurements," Phys. Rev. Lett. **98**, 223601 (2007).
8. E. Distante, M. Ježek, and U. L. Andersen, "Deterministic superresolution with coherent states at the shot noise limit," Phys. Rev. Lett. **111**, 033603 (2013).
9. Y. Gao, P. M. Anisimov, C. F. Wildfeuer, J. Luine, H. Lee, and J. P. Dowling, "Super-resolution at the shot-noise limit with coherent states and photon-number-resolving detectors," J. Opt. Soc. Am. B **27**, A170–A174 (2010).
10. L. Cohen, D. Istrati, L. Dovrat, and H. S. Eisenberg, "Super-resolved phase measurements at the shot noise limit by parity measurement," Opt. Express **22**, 11945–11953 (2014).
11. C. C. Gerry, "Heisenberg-limit interferometry with four-wave mixers operating in a nonlinear regime," Phys. Rev. A **61**, 043811 (2000).
12. A simple approach for increasing the fringe resolution by classical means is a multi-pass interferometer. As the mentioned techniques can be mapped to multi-pass configurations, we focus on the single-pass configuration.
13. J. Jacobson, G. Björk, I. Chuang, and Y. Yamamoto, "Photonic de Broglie waves," Phys. Rev. Lett. **74**, 4835–4838 (1995).
14. E. J. S. Fonseca, C. H. Monken, and S. Pádua, "Measurement of the de Broglie wavelength of a multiphoton wave packet," Phys. Rev. Lett. **82**, 2868–2871 (1999).
15. J. P. Dowling, "Correlated input-port, matter-wave interferometer: quantum-noise limits to the atom-laser gyroscope," Phys. Rev. A **57**, 4736–4746 (1998).
16. K. Jiang, H. Lee, C. C. Gerry, and J. P. Dowling, "Super-resolving quantum radar: coherent-state sources with homodyne detection suffice to beat the diffraction limit," J. Appl. Phys. **114**, 193102 (2013).
17. S. L. Braunstein and C. M. Caves, "Statistical distance and the geometry of quantum states," Phys. Rev. Lett. **72**, 3439–3443 (1994).
18. A. Monras, "Optimal phase measurements with pure Gaussian states," Phys. Rev. A **73**, 033821 (2006).
19. T. Nagata, R. Okamoto, J. L. O'Brien, K. Sasaki, and S. Takeuchi, "Beating the standard quantum limit with four-entangled photons," Science **316**, 726–729 (2007).
20. C. M. Caves, "Quantum-mechanical noise in an interferometer," Phys. Rev. D **23**, 1693–1708 (1981).
21. J. C. F. Matthews, X.-Q. Zhou, H. Cable, P. J. Shadbolt, D. J. Saunders, G. A. Durkin, G. J. Pryde, and J. L. O'Brien, "Towards practical quantum metrology with photon counting," npj Quantum Inf. **2**, 16023 (2016).
22. H. Grote, K. Danzmann, K. L. Dooley, R. Schnabel, J. Slutsky, and H. Vahlbruch, "First long-term application of squeezed states of light in a gravitational-wave observatory," Phys. Rev. Lett. **110**, 181101 (2013).
23. LIGO Scientific Collaboration, "Enhanced sensitivity of the LIGO gravitational wave detector by using squeezed states of light," Nat. Photonics **7**, 613–619 (2013).
24. D. Bouwmeester, "Quantum physics: high NOON for photons," Nature **429**, 139–141 (2004).
25. Y. Israel, S. Rosen, and Y. Silberberg, "Supersensitive polarization microscopy using NOON states of light," Phys. Rev. Lett. **112**, 103604 (2014).
26. P. M. Anisimov, G. M. Raterman, A. Chiruvelli, W. N. Plick, S. D. Huver, H. Lee, and J. P. Dowling, "Quantum metrology with two-mode squeezed vacuum: parity detection beats the Heisenberg limit," Phys. Rev. Lett. **104**, 103602 (2010).
27. I. Afek, O. Ambar, and Y. Silberberg, "High-NOON states by mixing quantum and classical light," Science **328**, 879–881 (2010).